# Spectral intermode coupling in a model of isotropic turbulence

T. Nakano,* W. D. McComb,† and B. J. Geurts‡
*Department of Physics and Astronomy, University of Edinburgh, Edinburgh EH9 3JZ, United Kingdom*
(Received 1 May 2002; published 27 February 2003)

We investigate the nonlinear coupling between the so-called *explicit* modes, identified with wave numbers $k$ such that $0 \leqslant k \leqslant k_c$, and *implicit* modes, defined such that $k_c \leqslant k \leqslant k_{max}$. Here $k_c$ is an arbitrarily chosen cutoff wave number and $k_{max}$ is the ultraviolet cutoff as determined by viscous damping. The stresses arising from the nonlinearity in the Navier-Stokes equations are categorized as ''implicit-implicit'' (or ''Reynolds'') and ''explicit-implicit'' (or ''cross''). These arise from dynamic coupling between different regions of wave number space. Their respective effects on momentum, kinetic energy, and energy flux are assessed. The analysis is based on a model system comprising the Navier-Stokes equations and the Edwards-Fokker-Planck energy equation [S. F. Edwards, J. Fluid Mech. **18**, 239 (1964)] which is known to retain all the symmetries of homogeneous, isotropic turbulence. The Reynolds stress is found to be responsible for long-range energy transfers. It can be represented by an effective viscosity and is mainly determined by dynamical friction. The cross term is more complicated, involving both diffusive and frictional effects. For long-range coupling it can be expressed as a modification of the effective viscosity, while for short-range coupling it may be modeled on the assumption that implicit scales are slaved to explicit scales. Thus, both the random and coherent aspects of intermode coupling in turbulent flows are relevant in the cross term. The imposition of a continuity requirement on energy transfer leads to a new parametrization that represents the effect of absent modes in a truncated spectral simulation, and takes into account the phase-coupling (coherent) effects, as well as the usual viscositylike (random) effects.

DOI: 10.1103/PhysRevE.67.026317 PACS number(s): 47.27.Gs

## I. INTRODUCTION

There is currently a great deal of interest in the study of physical systems that are governed by partial differential equations driven by noise or random forces. In the case of fluid turbulence, the controlling symmetry is the conservative exchange of energy among the Fourier wave number modes. This is a noteworthy feature because it imposes significant constraints on any attempt to reduce the number of degrees of freedom while retaining the primary flow features.

If we eliminate certain modes from the description, then in principle we must compensate in some way for the absent modes. In particular, it appears essential to at least maintain both the kinetic energy of the system and the rate at which energy is transferred through its modes. This problem has recently been studied by employing a conditional average to progressively eliminate modes in wave number shells, beginning with the highest wave numbers [1]. Each coarse-graining operation was followed by a rescaling, based on an effective turbulence viscosity that arises as a result of the conditional average. This sequence of operations was carried out in the viscous range of wave numbers $k$, where the Reynolds number based on $k$ is less than unity. This permits the unambiguous use of perturbation theory. The iteration is found to reach a fixed point that corresponds to the onset of scaling behavior (the so-called ''inertial range'' of wave numbers). Although the procedure is a form of renormalization group (RG), a clear distinction should be drawn between this approach and the use of RG in the study of driven hydrodynamics [2], along with later attempts by other workers to apply that work to turbulence: for a discussion of this aspect see the paper by Eyink [3].

In the present paper we approach the mode interaction and elimination problem from a different direction. We consider the Fourier modes of the velocity field $\mathbf{u}(\mathbf{k},t)$ on the wave number interval $0 \leqslant k \leqslant k_{max}$, where $k_{max}$ is chosen to be large enough to capture all the energy dissipation of the turbulence [1]. We divide the velocity field into $\mathbf{u}^{-}(\mathbf{k},t)$, for $0 \leqslant k \leqslant k_c$ (referred to as the explicit scales), and $\mathbf{u}^{+}(\mathbf{k},t)$ for $k_c \leqslant k \leqslant k_{max}$ (the implicit scales). The wave number cutoff $k_c$ is normally taken to be in the inertial range but is otherwise arbitrary. In particular, we examine the coupling between the explicit and implicit scales from the point of view of momentum, energy, and energy flux. Apart from its relevance from a fundamental point of view, this analysis can be used to formulate a parametrization of the dynamic consequences of small-scale turbulent motions on the evolution of large-scale flow features that are retained explicitly in a numerical simulation.

In order to study this problem, we represent the turbulence by a model system corresponding to the theory of Edwards [4]. This allows us to make both analytical and numerical predictions about the interscale coupling through integration of the energy transfer kernel over the appropriate regions of $k$ space and has the advantage over, e.g., direct numerical simulations that one can obtain results for arbitrarily large values of the Reynolds number. Moreover, contributions to the Reynolds and cross terms arising from different regions of $k$ space can be evaluated in detail.

However, in view of the interdisciplinary nature of turbu-

*Department of Physics, Chuo University, Tokyo.
†Email address: w.d.mccomb@ed.ac.uk
‡Faculty of Mathematical Sciences, University of Twente, The Netherlands.

 

lence research, it may be as well at this stage to clarify our use of the term ''model system.'' In physics it is usual to distinguish between *theories* that may involve approximations of a general kind, such as truncation of expansions at a consistent order, and *models* that involve more specific assumptions and which normally involve the introduction of one or more constants that must be fixed by comparison with experiment. In the context of turbulence, examples of *theories* include the direct-interaction approximation (DIA), the Edwards-Fokker-Planck theory (EFP), the self-consistent-field theory (SCF) and the local energy transfer theory (LET) whereas examples of *models* include the test-field model (TFM) and the eddy-damped quasinormal Markovian theory (EDQNM) [5,6]. In the context of engineering fluid dynamics the theoretical activity is referred to as ''modeling'' and in practice the distinction between theories and models is rarely, if ever, made. Nevertheless, in effect, the definition of the term ''model'' is the same in both cultures.

It is when we consider the use to which we put a model that a chasm yawns between the two cultures. In engineering (and many other scientific disciplines, including, sometimes, physics) a model (or mathematical model) is intended to describe an actual practical situation and is expected to have predictive ability. It is judged essentially by this criterion: can it predict outcomes in real situations? If it cannot, then it will be rejected.

In fundamental physics the situation is completely different, and models are often studied in their own right as interesting physical systems. At the macroscopic level, we have the recent development of interest in driven (stochastic) diffusion equations such as the Kardar-Parisi-Zhang (KPZ) equation (for example, see Ref. [7] and references therein). Over the last two decades this has had hundreds of citations. Originally it was believed that it could describe phenomena ranging from nonlinear deposition to bunching in traffic queues. Nowadays such beliefs have fallen away, yet it is still intensively studied as a system in its own right because it is tractable and possesses interesting features such as nonlinearity and dissipation.

It is in this spirit that we study the model system obtained by combining the Navier-Stokes equation with the moment closure propased by Edwards. We do not claim that the results will apply directly to pure Navier-Stokes turbulence. But we do argue that the results are interesting in their own right; and, as they are based on ideas of conservation and symmetry, that they provide a *strategy* that is worth trying in the case of turbulence as they suggest a way of taking into account the phase coherence effects that are neglected in the usual viscositylike models.[1]

It should also be emphasized that by choosing the theory proposed by Edwards [4] we are not asserting its superiority to other such theories. We have given a detailed and comparative account of the main turbulence theories elsewhere [5,6] and our choice of the Edwards theory is largely dictated by its comparative simplicity, although its relationship to fundamental concepts in statistical mechanics is also of interest.

The organization of this paper is as follows. In Sec. II we review the basic equations and formulate the problem more precisely. Section III presents and discusses the EFP model used to describe the energy dynamics. Analytical, asymptotic estimates for the energy transfer, obtained with this model, are collected in Sec. IV while a more comprehensive numerical study is presented in Sec. V. The consequences of this analysis for a large-eddy simulation are described in Sec. VI in which a subgrid model is proposed, consistent with the intermode coupling in the EFP model. This is followed by our conclusions in Sec. VII.

## II. THE BASIC EQUATIONS AND STATEMENT OF THE PROBLEM

In the context of fluid dynamics, turbulence presents either a moment closure problem, if one favors the use of statistical theory, or a problem of many length and time scales, if one attempts a direct numerical simulation of the Navier-Stokes equations (NSEs) on a computer [5,6]. Over the last few decades, there has been growing interest in a hybrid approach, known as large-eddy simulation. As the name suggests, the largest scales of the motion are simulated on a grid in real ($\mathbf{x}$) space, with a closure model being employed to account for the nonlinear coupling to the ''subgrid'' scales. Statistical theory may be adopted to obtain an appropriate closure model, but similarity considerations and rigorous properties of the turbulent stresses can also be used to arrive at suitable models [8,9].

In order to elucidate some fundamental aspects of the general problem of reducing the number of degrees of freedom to be simulated, we restrict our attention to turbulence that is both homogeneous and isotropic, and work in the wave number–time domain. We consider, in particular, the stationary case in which energy is supplied to the fluid at a rate $\varepsilon$, which is equal to the viscous dissipation. We specify that the energy is injected at low wave numbers. It is then transferred by nonlinear mixing to high wave numbers, where it is dissipated by viscosity. For sufficiently large values of the Reynolds number, there will be an intermediate range where the effects of input and dissipation can be neglected and where the energy is transferred through wave number space, on average, at a constant rate equal to $\varepsilon$. This is known as the inertial range of wave numbers.

The length scales for this problem are set by the physical size of the box containing the turbulence and, for a fluid with molecular viscosity $\nu$, by the Kolmogorov length scale $\eta = (\nu^3/\varepsilon)^{1/4}$. In a spectral representation, as adopted here, it is convenient to work with the Kolmogorov dissipation wave number $k_d$, where

$$k_d = \frac{1}{\eta} = \left( \frac{\varepsilon}{\nu^3} \right)^{1/4}. \tag{2.1}$$

This expression shows how the largest wave numbers depend on the parameters $\varepsilon$ and $\nu$. For the purposes of fully resolved numerical simulation of the Navier-Stokes equation the usual rule of thumb is to take the maximum wave number in the discrete representation equal to

[1]These remarks apply only to numerical simulation of isotropic homogeneous spectral turbulence and not, for instance, to the use of the Smagorinski model in real flows.

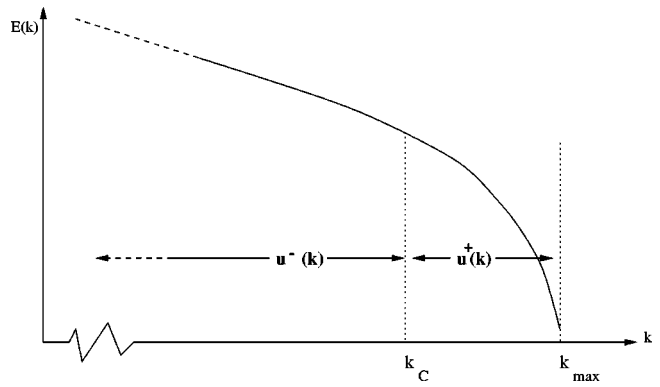


FIG. 1. A schematic view of the filtered fully resolved energy spectrum. In this work, we take $k_c$ to be somewhere in the inertial range of wave numbers.

$$k_{max} = 1.5 k_d .$$

A detailed numerical investigation of this point by McComb, Hunter, and Johnston [10] indicated that a slightly higher value $k_{max} \approx 1.8 k_d$ is needed in order to capture the dissipation in the system properly. It is also worth noting that the same investigation [10] revealed that if one cuts the turbulence off at a wave number $k_c = 0.5 k_d$, this would leave the turbulence energy $E$ virtually unaffected but would reduce the dissipation rate to about 40% of its correct value.

In Fig. 1 we show the universal, high wave number form of the spectrum schematically. We also indicate the low- and high-pass filtering of the velocity field into $\mathbf{u}^-(\mathbf{k})$ and $\mathbf{u}^+(\mathbf{k})$, corresponding to the resolved and subgrid scales, respectively. In Fig. 2 we show, also schematically, a truncated

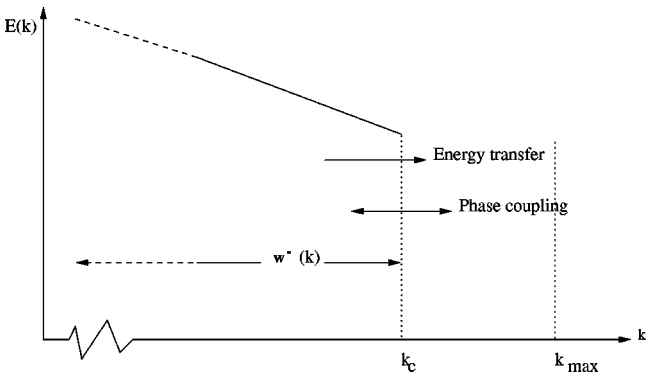


FIG. 2. Truncated energy spectrum.

spectrum corresponding to a large-eddy simulation in which the Fourier modes have been cut off somewhere inside the inertial range at $k = k_c$. The figure also indicates the boundary conditions that must be satisfied. First, it is necessary to represent the average energy flux through mode $k = k_c$. Second, the phase coupling between the resolved and subgrid modes should be taken into account. In the following sections we discuss the technical aspects of such a partial simulation, considering in turn conservation of momentum, conservation of energy, and the energy flux.

### A. The momentum equation

To study the large-eddy approach we require the low-pass filtered equation of motion for the velocity components with wave numbers less than $k_c$ (denoted by $-$). This equation also contains contributions from the subgrid modes (denoted by $+$). The filtered equation is obtained from the Navier-Stokes equation and can be written as

$$\left[\frac{\partial}{\partial t} + \nu k^2\right] u_\alpha^-(\mathbf{k}) = M_{\alpha\beta\gamma}(\mathbf{k}) \sum \delta_{\mathbf{k},\mathbf{j}+\mathbf{l}} [u_\beta^-(\mathbf{j}) u_\gamma^-(\mathbf{l}) + 2 u_\beta^+(\mathbf{j}) u_\gamma^-(\mathbf{l}) + u_\beta^+(\mathbf{j}) u_\gamma^+(\mathbf{l})], \tag{2.2}$$

where the $u^+u^+$ term is called the *Reynolds term*, while the $u^-u^+$ term will be referred to as the *cross term* hereafter. This is the solenoidal form of the Navier-Stokes equation in wave number space [5]. Greek indices take the values 1, 2, or 3 and the summation convention for repeated indices is employed. Note that in the interest of conciseness, we do not show the time dependence of the Fourier modes explicitly, but it is implied, e.g., that $u_\alpha^-(\mathbf{k}) = u_\alpha^-(\mathbf{k}, t)$. Following the usual practice, we use a symmetrized form of $M_{\alpha\beta\gamma}(\mathbf{k})$, thus

$$M_{\alpha\beta\gamma}(\mathbf{k}) = (2i)^{-1} [k_\beta D_{\alpha\gamma}(\mathbf{k}) + k_\gamma D_{\alpha\beta}(\mathbf{k})], \tag{2.3}$$

where the projector $D_{\alpha\beta}(\mathbf{k})$ is expressed in terms of the Kronecker delta as

$$D_{\alpha\beta}(\mathbf{k}) = \delta_{\alpha\beta} - \frac{k_\alpha k_\beta}{|\mathbf{k}|^2}. \tag{2.4}$$

As we shall see later, the cross term can be decomposed into two nonsymmetric forms (which in fact correspond to $\mathbf{u}^+ \cdot \nabla \mathbf{u}^-$ and $\mathbf{u}^- \cdot \nabla \mathbf{u}^+$, respectively, in real space).

The equation corresponding to the situation shown in Fig. 2 can be written in the form

$$\left[\frac{\partial}{\partial t} + \nu k^2\right] w_\alpha^-(\mathbf{k}) = M_{\alpha\beta\gamma}(\mathbf{k}) \sum \delta_{\mathbf{k},j+\mathbf{l}} w_\beta^-(\mathbf{j}) w_\gamma^-(\mathbf{l}) + F_\alpha[\mathbf{w}^-(\mathbf{k})], \tag{2.5}$$

where $F_\alpha[\mathbf{w}^-(\mathbf{k})]$ is a symbolic representation of the second and third nonlinear terms (i.e., the Reynolds and cross terms) on the right-hand side of Eq. (2.2). In practice, we reduce the number of degrees of freedom by choosing an approximate form of $F_\alpha[\mathbf{w}^-(\mathbf{k})]$, such that it represents the effect of the $\mathbf{u}^+(\mathbf{k})$ modes in some sense. In a truncated simulation we calculate $w_\alpha^-(\mathbf{k})$ on the interval $0 \leqslant k \leqslant k_c$, with values of $\varepsilon$

and $\nu$ such that $k_d \gg k_c$, and with initial condition obtained by reference to the full solution at some time $t_0$, thus

$$\mathbf{w}^-(\mathbf{k},0)=\mathbf{u}^-(\mathbf{k},t_0). \tag{2.6}$$

In principle, we can assess the accuracy of this partial simulation by comparing individual realizations with, and without, the high-wave-number modes being present. For this purpose we introduce a measure for the error $(\Delta_{\mathbf{k}})$ in mode $\mathbf{k}$ over a time interval $[t_0,t_0+T]$ by

$$\Delta_{\mathbf{k}}(T)=\max_{t_0<t\leqslant t_0+T}|\mathbf{u}^-(\mathbf{k},t)-\mathbf{w}^-(\mathbf{k},t)|, \tag{2.7}$$

where $\mathbf{u}^-(\mathbf{k},t)$ is the low-wave-number filtered part of the solution to Eq. (2.2) for the same values of $\epsilon$ and $\nu$. Essentially, this criterion tests the predictability of the low-$k$ modes, given some perturbation of the high-$k$ modes. The reverse problem—predictability of the high-$k$ modes given some perturbation of the low-$k$ modes—has been discussed in detail by Machiels [11].

Evidently, Eq. (2.5) is no longer the NSE (which would require all modes $0\leqslant k\leqslant k_{max}$ to be resolved) and the success or failure of Eq. (2.5) in satisfying $\Delta_{\mathbf{k}}(T)\leqslant\delta$, where $\delta$ is some error criterion, clearly depends on how well $F[\mathbf{w}^-(\mathbf{k})]$ represents the dynamical consequences of the small-scale flow features.

In principle, we should be able to choose an approximation to $F[\mathbf{w}^-(\mathbf{k})]$ such that the condition $\Delta_{\mathbf{k}}(T)\leqslant\delta$ is satisfied for arbitrarily small $\delta$. This follows from the classical determinism of the partial differential equation governing the fluid motion: the missing modes $\mathbf{w}^+(\mathbf{k})$ are predictable, at least in principle, given the $\mathbf{w}^-(\mathbf{k})$. Of course the price one would then pay is the need to solve the complete NSE for the $\mathbf{w}^+(\mathbf{k})$ and so there would be no computational saving. Thus it follows that some coarse-graining operation is necessary to obtain an approximation to $F[\mathbf{w}^-(\mathbf{k})]$ from the resolved modes $\mathbf{w}^-(\mathbf{k})$ and so reduce the size of the computational task, compared to obtaining $u^-$ from Eq. (2.2). In fact, it has recently been demonstrated that this coarse graining can be done algorithmically in a constrained numerical experiment [12], where a feedback loop gave rise to both eddy viscosity and eddy noise.

In general, one might hope to achieve a greater degree of coarse graining by means of some form of average. However, it is difficult to deal with the subgrid components in the momentum equation (2.2) directly, because of the nature of the averaging required. That is, one must average over subgrid modes $(u^+)$ while holding the explicit scales $(u^-)$ constant [1,13], and this involves the concept of a conditional average. We shall return to the question of how we should obtain an approximation to $F_\alpha[\mathbf{w}^-(\mathbf{k})]$ after we have considered the equations for the energy spectrum and the spectral energy flux.

### B. The energy equation

From the momentum equation we move on to the energy equation for the explicit modes, which is derived by multiplying each term of Eq. (2.2) by $u_\alpha^-(-\mathbf{k},t)$, and averaging over realizations of the $\mathbf{u}^-$. The result can be expressed as

$$\left[\frac{\partial}{\partial t}+2\nu k^2\right]E(k)=T(k)=T^{---}(k)+T^{--+}(k)+T^{-++}(k), \tag{2.8}$$

where

$$T^{---}(k)=2\pi k^2 M_{\alpha\beta\gamma}(\mathbf{k})\sum\ \delta_{\mathbf{k},\mathbf{j}+\mathbf{l}}\langle u_\alpha^-(-\mathbf{k})u_\beta^-(\mathbf{j})u_\gamma^-(\mathbf{l})\rangle+\text{c.c.}, \tag{2.9}$$

$$T^{--+}(k)=4\pi k^2 M_{\alpha\beta\gamma}(\mathbf{k})\sum\ \delta_{\mathbf{k},\mathbf{j}+\mathbf{l}}\langle u_\alpha^-(-\mathbf{k})u_\beta^-(\mathbf{j})u_\gamma^+(\mathbf{l})\rangle+\text{c.c.}, \tag{2.10}$$

$$T^{-++}(k)=2\pi k^2 M_{\alpha\beta\gamma}(\mathbf{k})\sum\ \delta_{\mathbf{k},\mathbf{j}+\mathbf{l}}\langle u_\alpha^-(-\mathbf{k})u_\beta^+(\mathbf{j})u_\gamma^+(\mathbf{l})\rangle+\text{c.c.}, \tag{2.11}$$

and c.c. stands for complex conjugate. Note that in each case the labeling wave number $k$ is restricted to the range $0\leqslant k\leqslant k_c$, so that this is the spectral energy equation for the explicit modes only.

Now, we wish to examine in particular the effects of $T^{--+}(k)$ and $T^{-++}(k)$ on $E(k)$ as a preliminary to considering how they should best be modeled. One particularly relevant aspect is to consider the conservation properties of this equation by using it to derive an expression for the energy flux across the cutoff wave number. We present this next, before actually focusing on the properties of $T^{--+}$ and $T^{-++}$ in Sec. III.

### C. The energy flux

As we saw in the context of Fig. 2, an important boundary condition that must be satisfied by a truncated spectral simulation is obtained by considering the average energy flux though the cutoff wave number $k_c$. We consider this in more detail now. By integrating Eq. (2.8) over $k$ from zero to $k_c$, we have

$$\frac{\partial}{\partial t}\int_0^{k_c}E(k)dk+2\nu\int_0^{k_c}k^2E(k)dk=-\Pi(k_c), \tag{2.12}$$

with the energy flux across wave number $k_c$ given by an integral over the explicit modes:

$$\Pi(k_c)=-\int_0^{k_c}dk[T^{---}(k)+T^{--+}(k)+T^{-++}(k)]=\Pi_{cross}(k_c)+\Pi_{reyn}(k_c). \tag{2.13}$$

Here the contribution from the first term in the integral vanishes due to symmetry, and the contributions from the cross term and the Reynolds term are given, respectively, by

$$\Pi_{cross}(k_c) = -\int_0^{k_c} T^{--+}(k)dk, \tag{2.14}$$

$$\Pi_{reyn}(k_c) = -\int_0^{k_c} T^{-++}(k)dk. \tag{2.15}$$

That is, $\Pi_{reyn}(k_c)$ is the energy transfer rate due to the Reynolds term, while $\Pi_{cross}(k_c)$ is the energy transfer rate due to the cross term.

### III. ENERGY EQUATION BASED ON CLOSURE THEORY

In order to estimate the order of magnitude of the Reynolds and cross terms, we shall rely on a model equation for the energy spectrum $E(k)$. This equation is derived on the basis of the closure theory proposed by Edwards [4], which is the EFP. This theory is known to retain all the symmetries of homogeneous, isotropic turbulence. As EFP also possesses good qualitative and quantitative behavior [5], we expect that our results will be representative of the full Navier-Stokes system. The advantage of the analytical model is that we can obtain results valid in the limit of large Reynolds numbers, which would be far beyond the range of fully resolved direct numerical simulations that are presently feasible. Moreover, through analysis we can evaluate the contributions to the various terms stemming from different regions of wave number space.

As shown in Appendix A, EFP leads to the form

$$\left[\frac{\partial}{\partial t} + 2\nu k^2\right] E(k) = T(k) = \int dl \int dj T(k,l,j), \tag{3.1}$$

where

$$T(k,l,j) = \frac{\pi^2}{klj} H(k,l,j) I(k,l,j)\, \theta(k,l,j) Q(l)[Q(j) - Q(k)], \tag{3.2}$$

$$H(k,l,j) = 2k^2j^2 + l^2(l^2 - k^2 - j^2), \tag{3.3}$$

$$I(k,l,j) = (k+l+j)(k+l-j)(k-l+j)(l+j-k), \tag{3.4}$$

$$\theta(k,l,j) = [\omega(k) + \omega(l) + \omega(j)]^{-1}. \tag{3.5}$$

In these expressions $\omega(k)$ is the rate of decay of mode $k$ and contains the renormalized or effective turbulent viscosity. Also, $Q(k)$ is the spectral density such that

$$E(k) = 4\pi k^2 Q(k).$$

We shall refer to the term $Q(l)Q(j)$ in Eq. (3.2) as the *diffusion term*. This term acts on mode $k$ as noise since its contribution may be positive or negative. The term $Q(l)Q(k)$ is (in the context of the Fokker-Planck equation) called the *dynamical friction term*, although for brevity we shall refer to it as the *friction term*. (The word ''viscosity'' will be kept for another purpose.)

The integration region for the variables $j$ and $l$ is the strip (see Fig. 3) bounded by

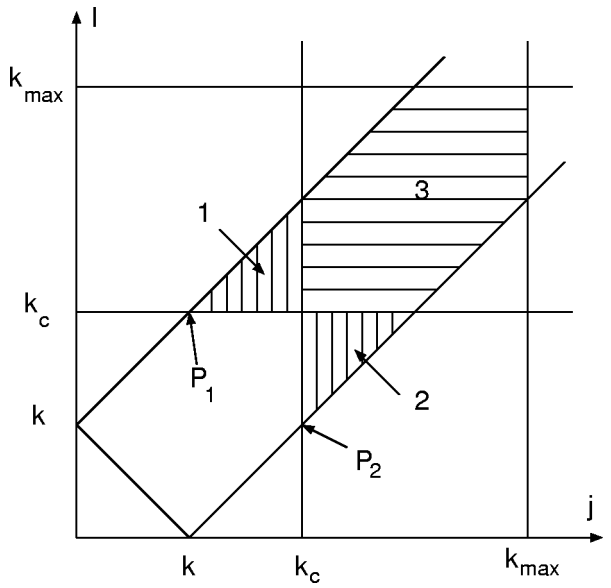


FIG. 3. The integration region of $T_{reyn}(k)$ is denoted by 3 while the integration region for $T_{cross}(k)$ is denoted by 1 and 2. Note that $P_1$ and $P_2$ are the significant points referred to in Sec. V A and Appendix C.

$$j + k \geqslant l \geqslant j - k, \quad j + l \geqslant k, \tag{3.6}$$

which is the condition that $k$, $j$, and $l$ make up the three sides of a triangle. The integration region that defines $T^{-++}$ [the Reynolds term $T_{reyn}(k|k_c)$] is $l,j > k_c$ which is marked as 3 in Fig. 3, where $k_{max}$ is the largest wave number. The integration region that specifies $T^{--+}$ [the cross term $T_{cross}(k|k_c)$] is $l \geqslant k_c$, $j \leqslant k_c$ or vice versa, marked as 1 and 2, respectively, in Fig. 3.

In order to clarify the energy dynamics arising from various regions in wave number space, we need to evaluate $T^{--+}$ and $T^{-++}$ by integrating $T(k,l,j)$ as given in Eq. (3.2) over the appropriate $j$ and $l$ regions. Specifically, these quantities are defined by

$$T_{reyn}(k|k_c) = T^{-++}(k) = \int_{k_c}^{k_{max}} dl \int_{k_c}^{k_{max}} dj\, T(k,l,j), \tag{3.7}$$

$$T_{cross}(k|k_c) = T^{--+}(k) = \left[\int_{k_c}^{k_{max}} dl \int_0^{k_c} dj + \int_0^{k_c} dl \int_{k_c}^{k_{max}} dj\right] T(k,l,j). \tag{3.8}$$

Before beginning our estimation of $T_{reyn}(k|k_c)$ and $T_{cross}(k|k_c)$, numerically in Sec. V as well as analytically in Sec. IV, we remark that $I$, as given by Eq. (3.4) is always positive. In contrast, $H$, as defined by Eq. (3.3) changes sign in the triangle strip. The dark region in Fig. 4 denotes the region where $H$ is negative. In the other area $H$ is positive. For this reason, the combination of $H(k,l,j)$ and $Q(j) - Q(k)$ determines the sign of the contribution to $T(k)$ from

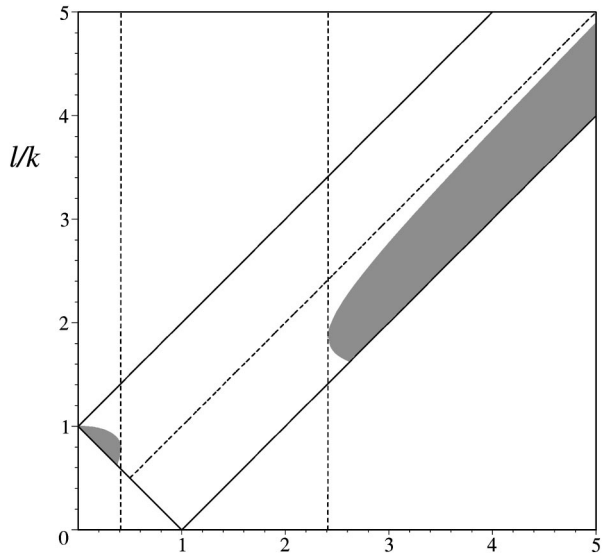


FIG. 4. Illustration of the behavior of $H$, as defined by Eq. (3.3), and plotted here as $H/k^4=2(j/k)^2+(l/k)^2[(l/k)^2-(j/k)^2-1]$. In the dark region $H$ is negative. Outside this region $H$ is positive. In this figure $(a)=\sqrt{2}-1$ and $(b)=\sqrt{2}+1$.

various regions of wave number space. In the Reynolds term, for instance, where $Q(j)-Q(k)<0$, the contribution from $j<l$ is mostly positive, while that from $j>l$ is negative. For an accurate evaluation a numerical calculation is needed to establish the final (negative) result.

## IV. ANALYTICAL ESTIMATES OF ENERGY TRANSFER

In this section we obtain analytical results for a number of limiting cases which clarify and support the subsequent numerical analysis and illustrations. We estimate the relative order of magnitude of the contribution to the ensemble-averaged closure of the Reynolds term with $k_c<j,l<k_{max}$ as compared to that of the cross term arising from regions 1 and 2 in Fig. 3. Since there is no agreed analytical result for the general form of the energy spectrum at a finite Reynolds number, our calculations are based on the inertial-range Kolmogorov spectrum only.

Here we estimate the contributions from the regions of integration specified as 1, 2 and 3 in Fig. 3. In order to estimate the right-hand side of Eq. (3.1) we rewrite it as

$$\left[\frac{\partial}{\partial t}+2\nu k^2\right]E(k)=\frac{\pi}{4k^3}[S(k)-R(k)Q(k)], \tag{4.1}$$

where

$$R(k)=\int dl\int dj\,\frac{1}{lj}H(k,l,j)I(k,l,j)\theta(k,l,j)Q(l), \tag{4.2}$$

$$S(k)=\int dl\int dj\,\frac{1}{lj}H(k,l,j)I(k,l,j)\theta(k,l,j)Q(l)Q(j). \tag{4.3}$$

In the following we consider two cases with $k\leqslant k_c$: (i) $k\ll k_c$ and (ii) $k\approx k_c$. Note that $R(k)$ is the dynamical friction (or friction for short) and $S(k)$ is the diffusion term.

### A. Asymptotic range: $k\ll k_c$

Referring to Fig. 3, we begin by considering region 3 and after that we consider regions 1 and 2 together.

#### 1. The Reynolds term: Region 3

We denote the contribution from Region 3 to $R$ and $S$ by the subscript ''3.'' The calculation was carried out using a Taylor expansion in powers of $k/k_c$. From Eqs. (4.12) and (4.13), and retaining the largest term, we obtain

$$R_3=\frac{8}{3}k^5\left[\int_{k_c}^{k_{max}}dl\left\{\frac{Q(l)}{\omega(l)}l^2\left(1+\frac{\alpha(l)}{5}\right)\right\}-\frac{1}{5}k_c^3\frac{Q(k_c)}{\omega(k_c)}\right], \tag{4.4}$$

$$S_3=\frac{8}{3}k^5\left[\int_{k_c}^{k_{max}}dl\left\{\frac{Q(l)^2}{\omega(l)}l^2\left(1+\frac{\beta(l)}{5}\right)\right\}-\frac{1}{5}k_c^3\frac{Q(k_c)^2}{\omega(k_c)}\right], \tag{4.5}$$

where

$$\alpha(l)=1+\frac{l\omega'(l)}{\omega(l)},\quad\text{and}\quad\beta(l)=\alpha(l)-2\frac{lQ'(l)}{Q(l)}. \tag{4.6}$$

In the inertial region $\alpha=5/3$, $\beta=9$, and

$$R_3=\frac{32}{15}k^5k_c^3\frac{Q(k_c)}{\omega(k_c)},\quad\text{and}\quad S_3=\frac{24}{25}k^5k_c^3\frac{Q(k_c)^2}{\omega(k_c)}. \tag{4.7}$$

The ratio $R(k)/k^5$ is the eddy viscosity. Comparing $S_3$ with $R_3Q(k)$, we have

$$\frac{S_3}{R_3Q(k)}=\frac{9}{20}\frac{Q(k_c)}{Q(k)}. \tag{4.8}$$

We note that the ratio on the left-hand side of Eq. (4.8) is small as long as $k\ll k_c$.

#### 2. The "cross term": Regions 1 and 2

The result of a similar calculation is

$$R_1+R_2=2\frac{Q}{\omega}k_c^2k^6\left[1+\frac{1}{6}\alpha(k_c)+\frac{1}{6}\left(\frac{Q}{\omega}\right)'\frac{\omega}{Q}k_c\right], \tag{4.9}$$

$$S_1+S_2=2\frac{Q^2}{\omega}k_c^2k^6\left[1+\frac{1}{6}\beta(k_c)+\frac{1}{6}\left(\frac{Q^2}{\omega}\right)'\frac{\omega}{Q^2}k_c\right]. \tag{4.10}$$

In the inertial range this becomes

$$R_1+R_2=\frac{10}{9}\frac{Q(k_c)}{\omega(k_c)}k_c^2k^6\quad\text{and}\quad S_1+S_2=\frac{7}{3}\frac{Q^2(k_c)}{\omega(k_c)}k_c^2k^6. \tag{4.11}$$

If we compare Eq. (4.11) with Eq. (4.7), then we have

$$\frac{R_1+R_2}{R_3}=\frac{25}{48}\frac{k}{k_c} \quad \text{and} \quad \frac{S_1+S_2}{S_3}=\frac{175}{72}\frac{k}{k_c}, \tag{4.12}$$

which indicates that the contribution of the cross term can be neglected when $k \ll k_c$.

In conclusion, the dominant contribution to the Reynolds term in the asymptotic range ($k \ll k_c$) comes from the friction. The diffusion contribution is smaller by a factor $Q(k_c)/Q(k)$ than the friction one. The cross term also receives contributions from friction and diffusion. However, both contributions are smaller than the corresponding contributions to the Reynolds term by a factor $k/k_c$. Both these conclusions, which are based on an order of magnitude estimation, would also hold true for a realistic spectrum at a finite Reynolds number, because a real viscous spectrum is known from experiment to fall off faster than a power with increasing wave number.

### B. Near-cutoff range: $k \approx k_c$

In this range, it is very difficult to estimate $R$ and $S$ in various regions analytically. However, we can establish the limiting values as $k$ goes to $k_c$. For $k \approx k_c$ we obtain

$$R_3 \sim R_1+R_2, \quad S_3 \sim S_1+S_2, \quad R_3 Q \sim S_3. \tag{4.13}$$

If we take into account the numerical prefactors obtained from the leading order in the Taylor expansion, $S_1+S_2$ appears to overwhelm the $S_3$ term as $k$ approaches the cutoff wave number $k_c$. Near the cutoff $k_c$ the contributions from the Reynolds term and the cross term will be of the same order of magnitude. In this region a more detailed comparison of the two must rely on numerical computation to which we turn in the following section.

## V. NUMERICAL EVALUATION OF ENERGY TRANSFER

In this section we focus on the separate energy transfer rates due to the Reynolds and cross terms. We cannot consider the individual contributions from the friction and diffusion separately, as for computational reasons it is necessary to work with the total kernel. This matter is explained in more detail in Appendix C, where we establish (for the Kolmogorov spectrum) that if the various contributions are computed separately, the integration in the cross term will diverge in the region $l \approx 0$ and $j \approx k$. Convergence relies on the vanishing of the factor $Q(j)-Q(k)$ as can be shown by expanding in powers of $l/k$. This is related to the well known fact that early closures were incompatible with the Kolmogorov spectrum, due to pathological behavior of the response integral [6], despite the fact that the energy equation was well behaved.

### A. Numerical computation

The integration region of $T_{reyn}(k|k_c)$ in Eq. (3.7) is region 3, as depicted in Fig. 3, which contains a large region in which $H$ is negative. The integration over $l$ and $j$ converges, so that the numerical evaluation is straightforward.

The integration region of $T_{cross}(k|k_c)$ in Eq. (3.8) consists of regions 1 and 2 in Fig. 3. Whether or not a negative region of $H$ is included in the integration region depends on the value of $k_c/k$. We must be careful with the integration in the vicinity of $l=0$ corresponding to the point $P_2$ in Fig. 3 and $j=0$ corresponding to the point $P_1$, which arises when $k \to k_c$. As shown in Appendix C, however, the contributions from those regions are negligible.

For the purposes of the numerical computation it is helpful to express $k$, $l$, and $j$ in terms of dimensionless variables $x$, $y$, and $z$, thus

$$k=k_c x, \quad l=k_c y, \quad j=k_c z. \tag{5.1}$$

To complete the description, the following forms of the energy spectrum $Q(k)$ and the modal decay rate $\omega(k)$ are introduced:

$$\begin{aligned} Q(k) &= (C/\pi)\varepsilon^{2/3}k^{-11/3}f(k/k_{max}) \\ &= (C/\pi)\varepsilon^{2/3}k_c^{-11/3}x^{-11/3}f(ax), \end{aligned} \tag{5.2}$$

$$\omega(k)=\sigma\varepsilon^{1/3}k^{2/3}g(k/k_{max})+\nu k^2=\sigma\varepsilon^{1/3}k_c{}^{2/3}x^{2/3}\zeta(ax), \tag{5.3}$$

$$\zeta(x)=g(x)+(bx)^{4/3}, \tag{5.4}$$

where $a=k_c/k_{max}$ and $b=k_{max}/\tilde{k}_d$ with $\tilde{k}_d=(\varepsilon\sigma^3/\nu^3)^{1/4}$, $C$ is the Kolmogorov prefactor (spectral constant), and $\sigma$ is the analogous constant in the inertial range form of the modal decay rate $\omega(k)$. The scaling functions $f(x)$ and $\zeta(x)$ are unity for $x \ll 1$ and decay exponentially for $x \gg 1$.

Substituting Eqs. (5.1)–(5.3) into Eqs. (3.7) and (3.8) yields

$$T_{reyn}(k|k_c)=k_c^{-1}\int_1^{a^{-1}}dy\int_1^{a^{-1}}dz\,T(x,y,z), \tag{5.5}$$

$$\begin{aligned} T_{cross}(k|k_c)=k_c^{-1}\Bigg[&\int_1^{a^{-1}}dy\int_0^{1}dz \\ &+\int_1^{a^{-1}}dy\int_0^{1}dz\Bigg]T(x,y,z), \end{aligned} \tag{5.6}$$

where

$$T(x,y,z)=\frac{C^2\varepsilon}{\sigma}\frac{1}{xyz}H(x,y,z)I(x,y,z),\frac{y^{-11/3}f(ay)[z^{-11/3}f(az)-x^{-11/3}f(ax)]}{x^{2/3}\zeta(ax)+y^{2/3}\zeta(ay)+z^{2/3}\zeta(az)}. \tag{5.7}$$

TABLE I. $T_{reyn}(k|k_c)$ and $T_{cross}(k|k_c)$ as functions of $x=k/k_c$. Note that each transfer term has been divided by the common factor $C^2\varepsilon/(k_c\sigma)$.

| $x$ | 0.01 | 0.05 | 0.1 | 0.2 | 0.3 | 0.5 | 0.8 | 0.9 | 1.0 |
|---|---|---|---|---|---|---|---|---|---|
| $-T_{reyn}(x)$ | 0.27 | 0.44 | 0.54 | 0.66 | 0.74 | 0.86 | 0.95 | 0.96 | 0.95 |
| $-T_{cross}(x)$ | 0.001 | 0.008 | 0.020 | 0.054 | 0.11 | 0.32 | 1.19 | 1.90 | 5.48 |

We base the following analysis of the energy transfer on this dimensionless formulation.

### B. Numerical analysis of energy transfer at infinite Reynolds number

We assume the infinite Reynolds number case, which implies that the Kolmogorov spectrum holds over the entire wave number space, and the scaling functions become $f(x)=\zeta(x)=1$. Obviously, more general forms of $f(x)$ and $\zeta(x)$ and a specific value of the parameter $a=k_c/k_{max}$ would be needed at a finite value of the Reynolds number. These aspects will not be considered here.

#### 1. $T_{reyn}(k|k_c)$ and $T_{cross}(k|k_c)$

The transfer spectra $T_{reyn}(k|k_c)$ and $T_{cross}(k|k_c)$ are listed in Table I as functions of $x=k/k_c$. As we are only interested in their relative magnitudes at this point, we have divided each of them by a common factor $C^2\varepsilon/(k_c\sigma)$. Note that $T_{cross}(k|k_c)$ is negligible in comparison to the Reynolds term as $x\to 0$ but overwhelms $T_{reyn}(k|k_c)$ for $k/k_c \geqslant 0.8$. This means that the cross interaction is important only near the cutoff. The decrease in $T_{cross}(k|k_c)$ as $k$ tends to zero is in agreement with the previous analytical estimates of the energy transfer for the case $k \ll k_c$ in section IV A.

We may use the energy transfer rate $T(k)$ to introduce the effective viscosity, as

$$\delta\nu(k) = -\frac{T(k)}{2k^2E(k)}. \tag{5.8}$$

Following a standard convention, we can express $\delta\nu(k)$ in terms of a dimensionless effective viscosity, denoted here by $X(k)$, thus

$$\delta\nu(k) = AX(k)\left[\frac{E(k_c)}{k_c}\right]^{1/2}, \tag{5.9}$$

where $A$ is a numerical constant. Figure 5 shows the effective viscosity $X(k)=x^{-1/3}T(x)$ for the total transfer rate $T=T_{reyn}+T_{cross}$. In the asymptotic region $k \ll k_c$ it is constant as expected, while in the vicinity of $k=k_c$ there is a cusp. In Fig. 5 we also include the effective viscosities from $T_{reyn}(k|k_c)$ and $T_{cross}(k|k_c)$ separately. It is noteworthy that $X_{reyn}(k)$ is almost independent of $k$: it decreases slightly as $k$ approaches the cutoff wave number $k_c$. On the other hand $X_{cross}(k)$ shows a cusp in the vicinity of $k=k_c$ in agreement with results from other investigations [10,14–16]. For $k \leqslant 0.7k_c$ the Reynolds-term viscosity is dominant.

Let us compare our computed $X(k)$ with some previous results. Kraichnan used the test field model [15] while Chollet and Leisure applied the very similar EDQNM [14]. We shall make a comparison with the work of the latter authors who gave an approximate expression for $X(k)$ as

$$X(k) = D'\{0.267 + 9.21\exp[-3.03(k_c/k)]\}, \tag{5.10}$$

where $D'$ is a numerical constant. We compared our predictions arising from EFP with Eq. (5.10) in Fig. 6. Here $D'$ is adjusted such that both results agree with each other in the asymptotic regime $k \ll k_c$. The solid line represents the present numerical calculation, and the dotted line corresponds to Eq. (5.10). Evidently, the qualitative agreement is reasonable while some quantitative differences remain.

It is also of interest to compare our findings with predictions obtained from direct numerical simulation. One such example is described by Domaradzki *et al.* [16], whose estimate of the viscosity (5.8) was based on DNS. However, since their simulation did not have an extended inertial region, the viscosity obtained did not have a proper asymptotic region for $k \ll k_c$ in which the viscosity tends to be constant. In fact, from the DNS it was observed that the viscosity could even become negative. Nevertheless, the cusp in the vicinity of $k=k_c$ was found to be a characteristic feature. Our result is consistent with this.

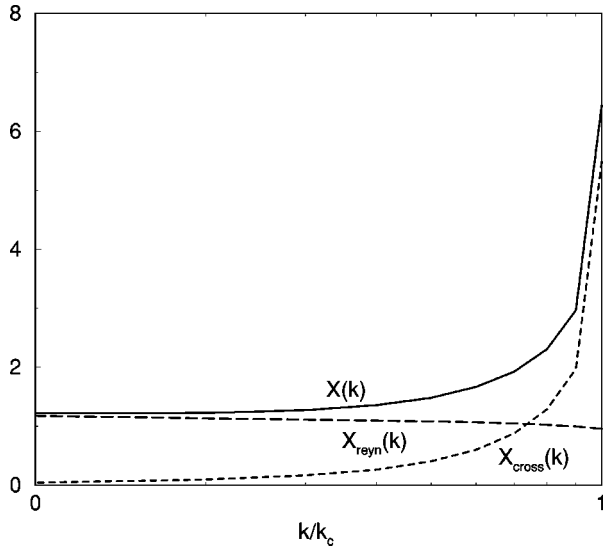


FIG. 5. Dimensionless effective viscosities $X(k)$, $X_{reyn}(k)$, and $X_{cross}(k)$ as defined by Eq. (5.9). Evidently the Reynolds term determines the asymptotic region $k/k_c \to 0$ while the cross term is responsible for the cusp.

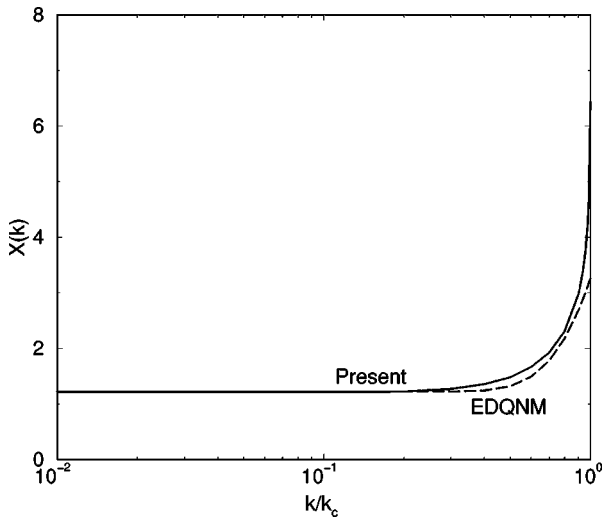


FIG. 6. Comparison of the present subgrid effective viscosity with the EDQNM [14] result.

### 2. Decomposition of $T_{reyn}(k|k_c)$

We further decomposed the effective viscosity $X_{reyn}(k)$ into *friction* and *diffusion* terms, denoting these by $X_{rf}$ and $X_{rd}$, respectively. We do this using the decomposition of $T_{reyn}$ into $R_3Q(k)$ and $S_3$, where $R_3$ and $S_3$ are given by Eq. (4.14) and (4.15), then invoking Eqs. (5.8) and (5.9) for the effective viscosity.

Since $X_{rd}$ is found to be negative, we have plotted $X_{rf}$ and $-X_{rd}$ in Fig. 7. It should be noted that $X_{rf}$ is much larger than $-X_{rd}$ in the entire wave number region, and that the magnitude of $-X_{rd}$ decreases very rapidly as $k$ decreases. The analytical estimates provided in Sec. IV A confirm the dominance of friction over diffusion as $k \ll k_c$. The numerical evaluation extends these estimates and shows that this property is maintained up to the region where $k \approx k_c$.

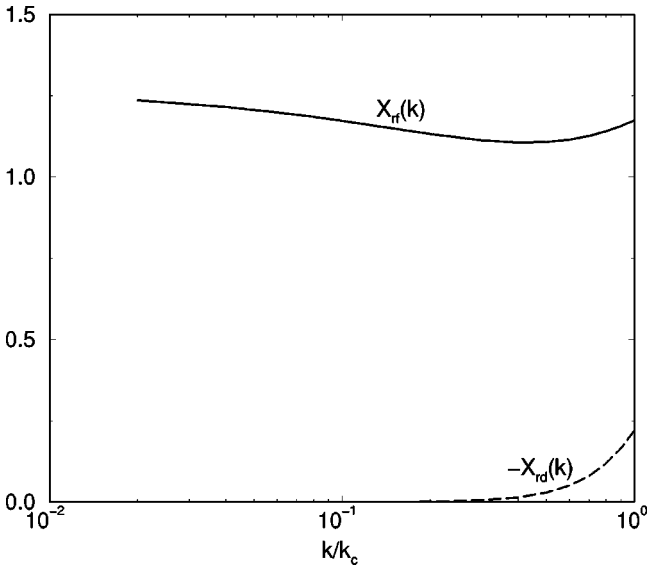


FIG. 7. Dimensionless effective viscosities $X_{rf}(k)$ and $X_{rd}(k)$, showing the relative contributions of the friction and diffusion terms to the Reynolds stress.

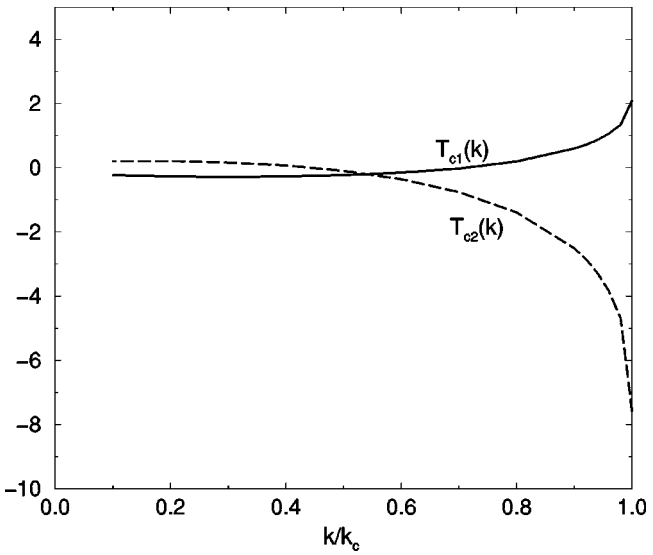


FIG. 8. Terms $T_{c1}(k)$ and $T_{c2}(k)$ as defined by Eqs. (5.12) and (5.13) corresponding to regions of integration 1 and 2, respectively, in Fig. 3. Evidently, $T_{c2}(k)$ is responsible for the ''cusp,'' consistent with the fact that by symmetry $T_{c1}(k)$ gives zero contribution to the flux through $k_c$: see Eq. (5.16).

### 3. Decomposition of $T_{cross}(k|k_c)$

The transfer rate associated with the cross term shows a cusp and in order to find out more about the origin of the cusp we first decomposed $T_{cross}(k|k_c)$ into two parts:

$$T_{cross}(k|k_c) = T_{c1}(k) + T_{c2}(k), \tag{5.11}$$

which correspond to the regions of integration 1 and 2, respectively, in Fig. 3, and where

$$T_{c1}(k) = \int_{k_c}^{\infty} dl \int_0^{k_c} dj \;\; T(k,l,j) \tag{5.12}$$

and

$$T_{c2}(k) = \int_{k_c}^{\infty} dj \int_0^{k_c} dl \;\; T(k,l,j), \tag{5.13}$$

with $T(k,l,j)$ as given by Eq. (3.2). We show $T_{c1}(k)$ and $T_{c2}(k)$ in Fig. 8 from which it is clear that the main source of the cusp in $T_{cross}(k)$ is $T_{c2}(k)$. This is not entirely surprising as we have

$$\int_0^{k_c} T_{c1}(k)dk = \int_{k_c}^{\infty} dl \int_0^{k_c} dj \int_0^{k_c} dk\, T(k,j,l) = 0, \tag{5.14}$$

since

$$T(k,j,l) = -T(j,k,l),$$

and so $T_{c1}(k)$ does not contribute to the energy transfer through $k_c$. Note that both components of $T_{cross}(k)$ change their sign as $k$ decreases.

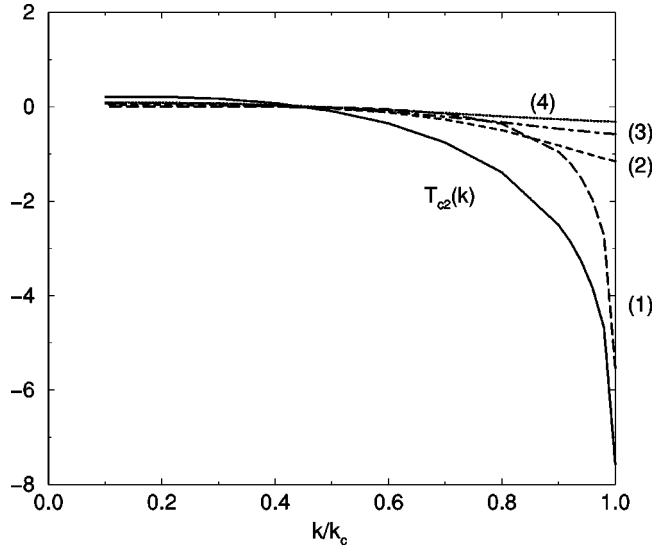


FIG. 9. Further decomposition of $T_{c2}(k)$ into contributions from different integration regions for wave numbers $l$, as discussed in Sec. V B3.

Since the cusp arises mainly from $T_{c2}(k)$ it is of interest to determine which part of region 2 in Fig. 3 contributes most to $T_{c2}(k)$. In order to determine the main interaction contributing to $T_{c2}(k)$, we divided the integration region for $l$ into four strips of equal width. That is, from Eq. (3.6) and Fig. 3, we may define region 2 as

$$k_c \geqslant l \geqslant k_c - k, \quad j \geqslant k_c .$$

This region is now further subdivided into four smaller strips defined as (1) $k_c - 0.75k \geqslant l \geqslant k_c - k$; (2) $k_c - 0.5k \geqslant l \geqslant k_c - 0.75k$; (3) $k_c - 0.25k \geqslant l \geqslant k_c - 0.5k$; (4) $k_c \geqslant l \geqslant k_c - 0.25k$. Figure 9 shows the contributions $T_{c2}^{(m)}(k)$ corresponding to integration over the individual segments $m = 1,2,3,4$ identified above. We see that the contribution from the first segment $T_{c2}^{(1)}(k)$ is responsible for the cusp in $T_{c2}(k)$. The contributions from the other segments are not only considerably smaller but in addition they are seen to vary rather smoothly. This result will be helpful when in Sec. VI we consider how the cross-term can best be modeled near the wave number cutoff.

### C. Energy flux across $k_c$

In this section we estimate the energy flux across the cutoff wave number $k_c$ numerically using the expression given in Eq. (2.13). We recall

$$\Pi_{reyn}(k_c) = -\int_0^1 T_{reyn}(x)dx$$

and

$$\Pi_{cross}(k_c) = -\int_0^1 T_{cross}(x)dx, \tag{5.15}$$

One can readily estimate $\Pi_{reyn}(k_c)$ and $\Pi_{cross}(k_c)$ by integrating $T_{reyn}(x)$ and $T_{cross}(x)$ over $x$. The result is

$$\Pi_{reyn}(k_c) = 0.80\frac{C^2\varepsilon}{\sigma} \quad \text{and} \quad \Pi_{cross}(k_c) = 0.68\frac{C^2\varepsilon}{\sigma}, \tag{5.16}$$

which indicates that $\Pi_{cross}(k_c)$ is comparable with $\Pi_{reyn}(k_c)$ for the inertial range spectrum, but $\Pi_{reyn}(k_c)$ is still the larger. Note that $\Pi_{cross}(k_c)$ is due to the single decomposition component $T_{c2}(k)$, as defined by Eq. (5.14), because the integration of $T_{c1}(k)$ gives a null result by symmetry.If we substitute the two expressions making up Eq. (5.16) into the boundary condition $\Pi(k_c) = \varepsilon$, we have

$$1.48\frac{C^2\varepsilon}{\sigma} = \varepsilon, \tag{5.17}$$

so that the numerical coefficient of the viscosity $\sigma$ is related to the Kolomogorov constant $K_0 = 4C$ as

$$\sigma = 1.48C^2 = 0.0925K_0^2. \tag{5.18}$$

If we use a currently accepted value of $K_0 = 1.6$, we find

$$\sigma = 0.24. \tag{5.19}$$

It is worth checking the correctness of the value obtained for $\Pi_{cross}(k_c)$ by employing another expression, originally derived by Kraichnan [17]. It is shown in Appendix D that the energy flux $\Pi_{cross}(k_c)$ can be converted to the expression

$$\Pi_{cross}(k_c) = \int_{k_c}^{\infty} dk \int_0^{k_c} dl \int_0^{k_c} dj\, T^{+--}(k,l,j). \tag{5.20}$$

Evaluating this expression we reached the same result as $\Pi_{cross}(k_c)$ in Eq. (5.16) which confirms our previous calculation.

In order to know how much of the energy in the wave number region less than $k$ is drained by the Reynolds and cross terms, we integrated $T_{reyn}(k')$ and $T_{cross}(k')$ over $0 \leqslant k' \leqslant k$:

$$\Pi_{reyn}(k) = -\int_0^{k/k_c} T_{reyn}(x')dx',$$
$$\Pi_{cross}(k) = -\int_0^{k/k_c} T_{cross}(x')dx', \tag{5.21}$$

and results for $\Pi_{reyn}(k)$ and $\Pi_{cross}(k)$ may be found in Fig. 10. From this figure we see that the Reynolds term contributes to the flux at any wave number, while the cross term only becomes important at wave numbers close to the cutoff. The cross term drains only a small amount of energy from wave numbers less than $k$ when $k \leqslant 0.5k_c$.

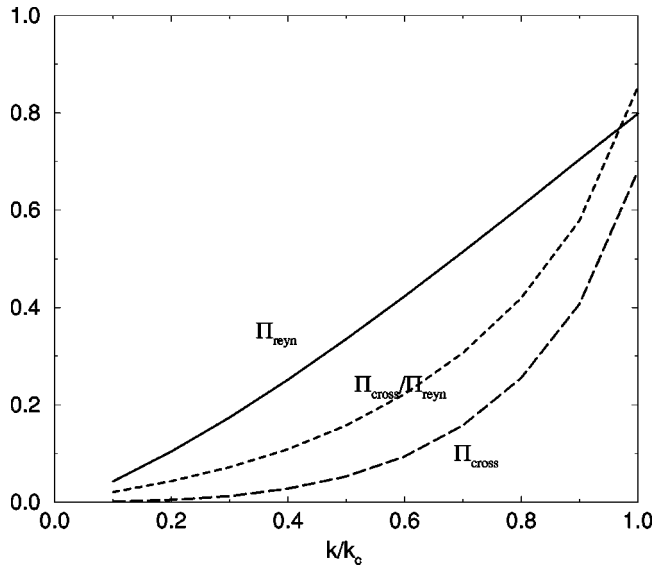


FIG. 10. $\Pi_{reyn}(k)$, $\Pi_{cross}(k)$, and their ratio.

## VI. FORMULATION OF A "LARGE-EDDY" SIMULATION

In this section we will put forward a model to represent the dynamic effects of modes with $k \geqslant k_c$ on the evolution of the explicit modes with $k \leqslant k_c$. This model will be based on our results for the Reynolds and cross terms obtained in the previous sections. The proposed model is required to represent the effects of the term $F_\alpha[\mathbf{w}^-(\mathbf{k})]$ which appears in the truncated momentum equation. In the first instance we will incorporate properties and considerations involving the spectral energy balance and flux, from which all phase information about the solution has been eliminated by construction. After that, the element of phase coupling will be addressed in Sec. VI B 2.

In order to do this we will find it convenient to first redefine the asymptotic and near-cutoff ranges of wave numbers in a more specific way than we did in Sec. IV. Let us suppose that $j > l$ for simplicity.

First we consider the case when $l > k_c$. Here both components are in the subgrid region and the subgrid stress is represented by the Reynolds term only. The situation is similar to the asymptotic range in Sec. IV.

Next turn to the case $l < k_c$: that is, the cross term. From Eq. (3.6) we have $l > j - k$, so the lowest value of wave number $l$ is $l_{min} = k_c - k$. Depending on whether $l_{min} > k$, that is, $k < k_c/2$; or $l_{min} < k$, that is, $k > k_c/2$, the situation is quite different. As can be seen from Table I, in the former case the energy transfer contribution from the cross term can be ignored as compared with the Reynolds term. In the latter case one cannot neglect the contribution of the cross term. As $k$ approaches $k_c$, the cross term overwhelms the Reynolds term.[2]

Hence it will be convenient to decompose the range of the resolved scales into two parts, viz., (1) The asymptotic range; $k \leqslant k_c/2$; (2) the near-cutoff range: $k \geqslant k_c/2$.

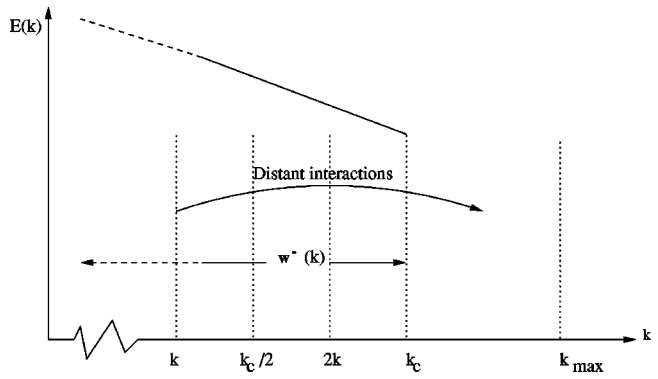


FIG. 11. For modes with $k < k_c/2$ only distant interactions are possible.

### A. The asymptotic range: $k \leqslant k_c/2$

In this range the interaction of the resolved scales with the subgrid scales can be regarded as a *distant interaction*, as illustrated in Fig. 11. The Reynolds term, as judged both by spectral energy balance (see Fig. 5) and by flux (see Fig. 10), is dominant over the cross term, and this suggests that it will also be dominant in the momentum equation for this range of wave numbers.

In addition, the fact that we have shown that the main contribution to energy transfer associated with the Reynolds stress comes from the dynamical friction, offers more fundamental support to the proposal that we should represent this term by an eddy viscosity. Hence we propose to include an effective eddy viscosity in Eq. (2.5). The coefficient of the eddy viscosity should be modified from an asymptotic value calculated for $k \ll k_c$, to a value depending on $k/k_c$, as shown in $X_{rf}(k)$ in Fig. 7.

The inclusion of the diffusion effect is subsidiary; but in practice it could prove quite helpful to include it. The required eddy viscosity is hence based on $X_{reyn}(k)$, as shown in Fig. 5. This is computed from $T_{reyn}(k)$, and is almost independent of $k$ in this (asymptotic) range of wave numbers.

### B. The near-cutoff range: $k_c/2 \leqslant k < k_c$

In this range, mode $k$ is affected by both local interactions where $k_c < j < 2k$ and distant interactions where $2k < j < k_{max}$, as shown in Fig. 12. Here we should make it clear how the term *local interaction* is used in the present paper. Some authors such as Ohkitani and Kida [18] have used the term to represent the interaction $k \approx l \approx j$ and in that context a term such as $l \ll k \approx j$ is called a distant interaction. In the present discussion we are concerned with the magnitude of $k$ and $j$ only. We refer to an interaction such as $k \ll j$ as a distant interaction, while an interaction such as $k \approx j$ is a local interaction. In this subsection we consider how the stresses can be treated in order to represent both distant and local interactions.

#### 1. Distant interactions: $2k < j < k_{max}$

In this model, as we saw in Sec. IV A, the distant interactions are mainly represented by the dynamical friction part

[2]This is actually a slight overstatement and we shall make a more careful assessment of this point in Sec. VI D 3.

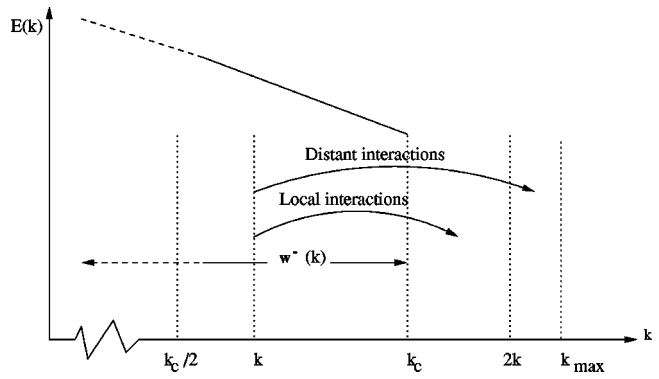


FIG. 12. For modes with $k>k_c/2$ both distant and local interactions are possible.

of the Reynolds term. Thus the arguments put forward in Sec. IV A for the asymptotic range $k\leqslant k_c/2$ will also hold for the distant interactions in the near-cutoff range with $k_c/2 \leqslant k\leqslant k_c$. In practice, one might encounter problems if $k_{max}$ is not much larger than $2k$, or if the energy spectrum decays very rapidly with wave number, as encountered in the dissipative region. Then the asymptotic form of the viscosity would need to be modified. However, this amounts to a restriction on the choice of $k_c$ as compared to $k_{max}$. In the typical case $k_{max}\gg 2k_c$. Accordingly, the use of a constant viscosity resulting from the Reynolds term seems appropriate, and this is supported by the results for $X_{reyn}(k)$, as shown in Fig. 5.

#### *2. Local interactions: $k_c<j<2k$*

From both Fig. 5 and Table I we can see that the cross term dominates as $k\rightarrow k_c$. This suggests that the cross term is mainly responsible for the local interactions and this is easily shown as follows. As we saw in Sec. V B 3, the most important contribution from the cross term is $T_{c2}(k)$; and, in particular, the contribution from small values of $l$ in the integral. From Eq. (5.13) for $T_{c2}$, we note that as $k\rightarrow k_c$ and $l\rightarrow 0$, the triangle condition requires $j\rightarrow k_c$. Hence only local interactions are involved.

As the Reynolds term has been shown to take care of the distant interactions, which is the ''random'' aspect of the coupling, it seems logical to assume that the local interactions represent the ''deterministic'' aspect, and this provides us with a hint as to how we should model it.

The following proposal seems to be the simplest model that is consistent with the findings from the numerical analysis in Sec. V. Obviously the success of any model can be tested only by examining simulation results obtained with it, and this is the subject of ongoing research.

We propose to approximate $u_\beta^+(\mathbf{j},t)$ by using the arbitrary resolved-scale velocity field $u_\beta^-(\mathbf{q},t)$ and assuming a deterministic connection between the two. Writing $u_\beta^+(\mathbf{j},t)$ as

$$u_\beta^+(\mathbf{j},t)=u_\beta^-(\mathbf{q},t)+[u_\beta^+(\mathbf{j},t)-u_\beta^-(\mathbf{q},t)], \tag{6.1}$$

we want to make the error, that is, the second term on the right-hand side in Eq. (6.1), as small as possible. If the error is Taylor expanded, we have

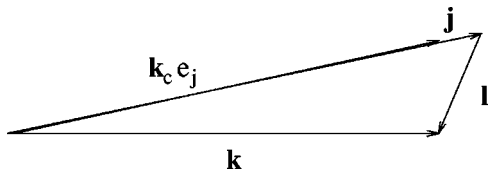


FIG. 13. Triangle of wave vectors representing the cross term. Here $\mathbf{e_j}$ is the unit vector along $\mathbf{j}$.

$$u_\beta^+(\mathbf{j},t)-u_\beta^-(\mathbf{q},t)=(\mathbf{j}-\mathbf{q})\cdot\nabla_{\mathbf{q}}u_\beta^-(\mathbf{q},t). \tag{6.2}$$

Then the error is expected to become small when $|\mathbf{j}-\mathbf{q}|$ is small. This is realized when $k_c\hat{\mathbf{j}}$ is chosen as $\mathbf{q}$ with $\hat{\mathbf{j}}$ being a unit vector along $\mathbf{j}$, where

$$\mathbf{j}-\mathbf{q}=\mathbf{j}-k_c\hat{\mathbf{j}}=\left(1-\frac{k_c}{j}\right)\mathbf{j}. \tag{6.3}$$

The wave vector configuration in such a case is depicted in Fig. 13, where $l$ is much smaller than $k_c$ and $j$ is slightly larger than $k_c$. This is the most important configuration contributing to the cross term as confirmed by the decomposition of $T_{c2}(k)$: see Sec. V B 3 and Fig. 9.

We further propose that in the case of the near interaction in the cross term:

$$M_{\alpha\beta\gamma}(\mathbf{k})\sum_{\mathbf{j}}\ \delta_{\mathbf{k},\mathbf{j}+\mathbf{l}}u_\beta^+(\mathbf{j},t)u_\gamma^-(\mathbf{l},t), \tag{6.4}$$

$u_\beta^+(\mathbf{j},t)$ is approximated by the velocity field nearest in the wave vector space to the velocity field on a resolved scale:

$$\tilde{u}_\beta^+(\mathbf{j},t)=\mu u_\beta^-(k_c\hat{\mathbf{j}},t)G(j/k_c)=\mu w_\beta^-(k_c\hat{\mathbf{j}},t)G(j/k_c), \tag{6.5}$$

where $G(j/k_c)$ signifies how the amplitude should be modified depending on where $k_c$ and $j$ are located. Here $\mu$ is a constant factor taking into account any possible phase mismatch, so that it is less than or equal to unity. For simplicity, we shall assume that it is unity. If $j$ is in the inertial range, then

$$G^2(j/k_c)=(j/k_c)^{-11/3}. \tag{6.6}$$

The advantages of the above approximation may be stated as follows. Proper models for the parametrization of the effects of the small scales should also include phase coupling between the explicit and the implicit modes. The phase effects are considered to a certain extent in this model, because the phase of $u_\beta^+(\mathbf{j},t)$ is expected to be not so different from that of $u_\beta^-(k_c\hat{\mathbf{j}},t)$. The phase effect signifies that the modeled term works as a forward transfer of energy for some of the time and a backward transfer of energy at other times.

### C. Proposed "subgrid" model

In this subsection we propose a model for the momentum equation based on the preceding energy considerations.

#### *1. Asymptotic range: $k \leqslant k_c/2$*

In the first instance, we assume that the cross term does not contribute to energy transfer in this wave number range. Hence Eq. (2.5) can be written as

$$\left[\frac{\partial}{\partial t}+\nu k^2\right] w_\alpha^-(\mathbf{k},t) = M_{\alpha\beta\gamma}(\mathbf{k}) \sum \delta_{\mathbf{k},\mathbf{j}+\mathbf{l}} w_\beta^-(\mathbf{j},t) w_\gamma^-(\mathbf{l},t) - \nu_r(k|k_c) k^2 w_\alpha^-(\mathbf{k},t). \tag{6.7}$$

The eddy viscosity $\nu_r(k|k_c)$ is taken to be due to the entire Reynolds term[3] represented by Eq. (5.9) with constant $X_{reyn}$ and is

$$\nu_r(k|k_c) = \sigma \varepsilon^{1/3} k_c^{-4/3} = \sigma K_0^{-1/2} \left(\frac{E(k_c)}{k_c}\right)^{1/2} = 0.2 \left(\frac{E(k_c)}{k_c}\right)^{1/2}, \tag{6.8}$$

where we have also made use of Eq. (5.8). Note that once we have considered the need for continuity with the model in the near-cutoff range, we shall modify this equation to the form given later in Eq. (6.17).

#### *2. Near-cutoff range: $k_c/2 \leqslant k < k_c$*

In this wave number range the cross term is roughly of the same order of magnitude as the Reynolds term, as far as the energy is concerned. Hence we propose a mixed model consisting of the viscosity plus the similarity term approximated by Eq. (6.5).

In order to write the model equation we have to know which cross term must be kept. The cross term in the equation for $u_\alpha^-(\mathbf{k},t)$ in Eq. (2.2) has two parts:

$$-i \sum_{\mathbf{j},\mathbf{l}} \delta_{\mathbf{k},\mathbf{j}+\mathbf{l}} [k_\gamma D_{\alpha\beta}(\mathbf{k}) u_\beta^+(\mathbf{j},t) u_\gamma^-(\mathbf{l},t) + k_\beta D_{\alpha\gamma}(\mathbf{k}) u_\beta^+(\mathbf{j},t) u_\gamma^-(\mathbf{l},t)]. \tag{6.9}$$

The energy contribution is obtained by multiplying Eq. (6.9) by $u_\alpha^-(-\mathbf{k},t)$ and averaging, as before, over realizations:

$$-i \sum_{\mathbf{j},\mathbf{l}} \delta_{\mathbf{k},\mathbf{j}+\mathbf{l}} [\langle \mathbf{u}^-(-\mathbf{k},t) \cdot \mathbf{u}^+(\mathbf{j},t) \mathbf{k} \cdot \mathbf{u}^-(\mathbf{l},t) \rangle + \langle \mathbf{u}^-(-\mathbf{k},t) \cdot \mathbf{u}^-(\mathbf{l},t) \mathbf{k} \cdot \mathbf{u}^+(\mathbf{j},t) \rangle]. \tag{6.10}$$

When we further consider the energy transfer, the second term in Eq. (6.10) vanishes upon integration over $\mathbf{k}$, so that it corresponds to $T_{c\mathbf{1}}(k)$. From these considerations we infer that we should retain the first term in Eq. (6.9) as the necessary cross term:

$$-i \sum_{\mathbf{l},\mathbf{j}} \delta_{\mathbf{k},\mathbf{l}+\mathbf{j}} k_\gamma D_{\alpha\beta}(\mathbf{k}) u_\beta^+(\mathbf{j},t) u_\gamma^-(\mathbf{l},t). \tag{6.11}$$

Then we can express Eq. (2.5) as

$$\left[\frac{\partial}{\partial t}+\nu k^2\right] w_\alpha^-(\mathbf{k},t) = M_{\alpha\beta\gamma}(\mathbf{k}) \sum \delta_{\mathbf{k},\mathbf{j}+\mathbf{l}} w_\beta^-(\mathbf{j},t) w_\gamma^-(\mathbf{l},t) - \nu_r(k|k_c) k^2 w_\alpha^-(\mathbf{k},t) - i \sum_{\mathbf{l},\mathbf{j}} \delta_{\mathbf{k},\mathbf{l}+\mathbf{j}} k_\gamma D_{\alpha\beta}(\mathbf{k}) \tilde{u}_\beta^+(\mathbf{j},t) w_\gamma^-(\mathbf{l},t), \tag{6.12}$$

where $\tilde{u}_\beta^+(\mathbf{j},t)$ is given by Eq. (6.5). However, since the term

$$\sum_{\mathbf{l},\mathbf{j}} \delta_{\mathbf{k},\mathbf{l}+\mathbf{j}} k_\beta D_{\alpha\gamma}(\mathbf{k}) \tilde{u}_\beta^+(\mathbf{j},t) w_\gamma^-(\mathbf{l},t) \tag{6.13}$$

does not contribute to the energy we include Eq. (6.13) in Eq. (6.12) which has the benefit of keeping the model equation symmetrical. In total, the proposed model equation for $k \geqslant k_c/2$ is

$$\left[\frac{\partial}{\partial t}+\nu k^2\right] w_\alpha^-(\mathbf{k},t) = M_{\alpha\beta\gamma}(\mathbf{k}) \sum \delta_{\mathbf{k},\mathbf{j}+\mathbf{l}} w_\beta^-(\mathbf{j},t) w_\gamma^-(\mathbf{l},t) - \nu_r(k|k_c) k^2 w_\alpha^-(\mathbf{k},t) + 2 M_{\alpha\beta\gamma}(\mathbf{k}) \sum_{\mathbf{l},\mathbf{j}} \delta_{\mathbf{k},\mathbf{l}+\mathbf{j}} \tilde{u}_\beta^+(\mathbf{j},t) w_\gamma^-(\mathbf{l},t). \tag{6.14}$$

#### *3. Continuity at $k = k_c/2$*

Finally, we want to formulate the full model such that expressions (6.12) and (6.14) are continuous at $k = k_c/2$. The difference is only the last term in Eq. (6.14), which yields $T_{cross}(k = k_c/2)$ as far as the energy is concerned. Table I indicates that the ratio of $T_{cross}(k)$ to $T_{reyn}(k)$ is 0.37, so, although $T_{reyn}(k)$ is larger than $T_{cross}(k)$, the latter is certainly not negligible. To compensate for it, we should add a contribution from the cross term to Eq. (6.7) in the form of the additional eddy viscosity

$$-\nu_c(k|k_c) k^2 w_\alpha^-(\mathbf{k},t), \tag{6.15}$$

where $\nu_c(k|k_c)$ is the eddy viscosity due to the cross term.[4] As can be seen from Fig. 5, $\nu_c(k|k_c)$ decreases as $k/k_c$ does. Its dependence on $k/k_c$ can be estimated from its asymptotic form. As we saw earlier the contribution from the cross term is a factor $k/k_c$ smaller than the Reynolds term, so that $\nu_c(k|k_c) \propto k/k_c$. Therefore we put

$$\nu_c(k|k_c) = 0.74 (k/k_c) \nu_r(k/k_c), \tag{6.16}$$

where the coefficient is selected in such a way that $\nu_c(k|k_c)/\nu_r(k|k_c) = 0.37$ at $k = k_c/2$.

[3] This is preferable, because it is almost independent of wave number.

[4] In the asymptotic region $0 \leqslant k \leqslant k_c/2$ the cross term also behaves like a viscous term.

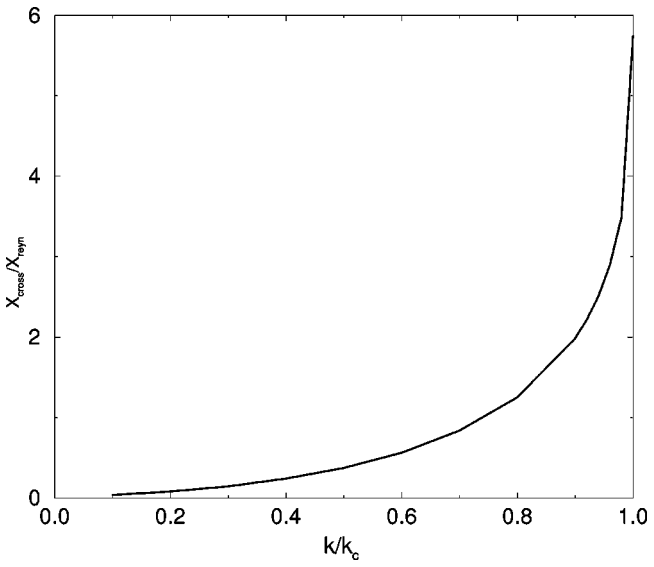


FIG. 14. Ratio of $X_{cross}(k)$ to $X_{reyn}(k)$.

With this in mind, the model equation for $k<k_c/2$ as given by Eq. (6.7), is now replaced by

$$\left[\frac{\partial}{\partial t}+\nu k^2\right]w_\alpha^-(\mathbf{k},t)=M_{\alpha\beta\gamma}(\mathbf{k})\sum\ \delta_{\mathbf{k},\mathbf{j}+\mathbf{l}}w_\beta^-(\mathbf{j},t)w_\gamma^-(\mathbf{l},t)-\nu_r(k|k_c)(1+0.74k/k_c)k^2w_\alpha^-(\mathbf{k},t). \tag{6.17}$$

#### *4. Optimization*

In the model just given we have divided the wave number region into two parts at $k=k_c/2$. Although this choice of a dividing wave number is intuitively plausible it is also arbitrary. In practice, it may be better to adopt a more general approach and choose as the dividing wave number $k=\lambda k_c$, where $\lambda$ is a constant, such that $0\leqslant\lambda\leqslant 1$, which may be treated as an optimization parameter. Then for $k\leqslant\lambda k_c$ we have

$$\left[\frac{\partial}{\partial t}+\nu k^2\right]w_\alpha^-(\mathbf{k},t)=M_{\alpha\beta\gamma}(\mathbf{k})\sum\ \delta_{\mathbf{k},\mathbf{j}+\mathbf{l}}w_\beta^-(\mathbf{j},t)w_\gamma^-(\mathbf{l},t)-\nu_r(k|k_c)[1+\mathcal{F}(\lambda)k/k_c]k^2w_\alpha^-(\mathbf{k},t). \tag{6.18}$$

Here $\mathcal{F}(\lambda)$ is determined in such a way that the energy transfer rate is continuous at $k=\lambda k_c$:

$$\mathcal{F}(\lambda)=\frac{X_{cross}(\lambda)}{\lambda X_{reyn}(\lambda)}, \tag{6.19}$$

where $X_{cross}(k/k_c)/X_{reyn}(k/k_c)$ is given in Fig. 14. For $k\geqslant\lambda k_c$ we have the same equation as Eq. (6.14). It should be noted that if the value of $\lambda$ is chosen too large, we may not use the asymptotic form of $\nu_c(k|k_c)$ proportional to $k/k_c$ such as Eq. (6.16).

Lastly, we consider the physical significance of the dividing wave number $\lambda k_c$. In view of the preceding discussions, the magnitude of $\lambda$ measures how much the cross term is taken account of in the form of eddy viscosity. Larger values of $\lambda$ mean that the cross term is represented to a greater extent by the eddy viscosity. Smaller values of $\lambda$ signify that the more general dynamical effects of the cross term are taken into account.

## VII. CONCLUSION

The essential difficulty of the turbulence problem is often characterized as being the interplay between randomness and coherence. A purely random problem could be solved by the methods of statistical mechanics while a purely coherent problem would be deterministic and hence treatable by the methods of classical mechanics. In considering how to reduce the number of degrees of freedom in a numerical simulation of the Navier-Stokes equations, we have used the Edwards-Fokker-Planck energy equation as a guide to the modeling. This allowed us to identify which subgrid stresses can be modeled as if of purely random origin and which subgrid stresses can be plausibly treated as deterministic. In the former case, we introduce an effective eddy viscosity; in the latter case we assume that subgrid modes are slaved to explicit modes. This procedure is facilitated by dividing the explicit scales into two wave number ranges, with a corresponding modeled equation of motion for each. In this way we can retain the primary effects arising from the nonlinear coupling between explicit (or resolved) modes and implicit (or subgrid) modes.

Specifically, for $k<k_c/2$, we have Eq. (6.17), which we repeat here for convenience:

$$\left[\frac{\partial}{\partial t}+\nu k^2\right]w_\alpha^-(\mathbf{k},t)=M_{\alpha\beta\gamma}(\mathbf{k})\sum\ \delta_{\mathbf{k},\mathbf{j}+\mathbf{l}}w_\beta^-(\mathbf{j},t)w_\gamma^-(\mathbf{l},t)-\nu_r(k|k_c)(1+0.74k/k_c)k^2w_\alpha^-(\mathbf{k},t).$$

Also, for $k\geqslant k_c/2$, the model equation is Eq. (6.14), thus

$$\left[\frac{\partial}{\partial t}+\nu k^2\right]w_\alpha^-(\mathbf{k},t)=M_{\alpha\beta\gamma}(\mathbf{k})\sum\ \delta_{\mathbf{k},\mathbf{j}+\mathbf{l}}w_\beta^-(\mathbf{j},t)w_\gamma^-(\mathbf{l},t)-\nu_r(k|k_c)k^2w_\alpha^-(\mathbf{k},t)+2M_{\alpha\beta\gamma}(\mathbf{k})\sum_{\mathbf{l},\mathbf{j}}\ \delta_{\mathbf{k},\mathbf{l}+\mathbf{j}}\tilde{u}_\beta^+(\mathbf{j},t)w_\gamma^-(\mathbf{l},t), \tag{7.1}$$

where $\tilde{u}_\beta^+(\mathbf{j},t)$ is given by Eq. (6.5). In both equations, $\nu_r(k|k_c)$ is given by Eq. (6.8).

Of course, this set of equations is only valid for the model system obtained by combining the Navier-Stokes equation with the EFP equation for the energy transfer. For instance, we identified the separate energy flux due to $\Pi_{reyn}$ and $\Pi_{cross}$ in Eq. (5.16). Substituting the result for the constant $\sigma$ in Eq. (5.18) into the two relationships of Eq. (5.16) results in the values:

$$\Pi_{reyn}(k_c)=0.54\varepsilon \quad \text{and} \quad \Pi_{cross}=0.46\varepsilon.$$

Presumably, these particular numbers are characteristic of the EFP closure and we conjecture[5] that for pure Navier-Stokes turbulence both fluxes will be exactly equal to $0.5\varepsilon$.

Evidently, this set of equations can only be assessed for Navier-Stokes turbulence by actually using them to perform a partially resolved (or large-eddy) simulation and comparing the results to those from a fully resolved simulation with the same initial conditions as far as the large scales are concerned. This will be the subject of further work and in which we will also explore the optimized form that is obtained when we replace Eq. (6.17) by Eqs. (6.18) and (6.19).

Naturally, we hope that this investigation will lead to techniques that are of practical value in the study of fluid turbulence but at the same time we hope to shed more light on the underlying structure of the EFP [4]. Renormalized perturbation theories of this kind have suffered unjustified neglect for many years and EFP is of particular interest in that it has a strong physical basis and is founded on the well-known fact that single-point velocity distributions in turbulence depart only slightly from the Gaussian form. One reason for this neglect is the difficulty involved in testing such theories in practical situations that invariably involve both anisotropy and inhomogeneity. The application to the modeling problem in large-eddy simulation may be one way round this difficulty, as the small eddies can often be taken as isotropic and homogeneous.

Lastly, we mentioned at the outset that we have previously approached the present problem using the method of iterative conditional averaging [1]. Numerical assessments of that work have been given elsewhere [10]. In that approach, we work with a conditional average of what is here called the Reynolds term. We have made it clear that this conditional mode elimination can only contribute to a renormalized dissipation rate and does not fully include phase-coupling effects. The view was expressed [1,10] that, despite the fact that the ''cross term'' does not contribute to the conditional average, the dissipation rate is determined to a good approximation by the RG-type procedure. This was supported by a calculation of the Kolmogorov prefactor [1].

In the present work we see that the ''cross term'' and the Reynolds term make similar contributions to the energy transfer rate [see Eq. (5.16)]. The two situations may not be directly comparable. Here we eliminate modes, such that $k_c \leqslant k \leqslant k_{max}$, in one operation. In the conditional mode elimination [1] we eliminate modes progressively in shells, rescaling between each elimination. This point requires elucidation and will be the subject of further work.

## APPENDIX A: THE EQUATION FOR THE ENERGY SPECTRUM

In order to estimate the order of magnitude of the Reynolds term and the cross term we examine the energy equation obtained by a closure approximation. According to (E20) in McComb's book [6] the equation for the energy spectrum $E(k)=4\pi k^2 Q(k)$ becomes

$$\left(\frac{\partial}{\partial t}+2\nu k^2\right)E(k)=T(k)=4\pi k^2\int d^3j\int d^3l\;\delta(\mathbf{k}-\mathbf{j}-\mathbf{l})\times 2B(\mathbf{j},\mathbf{k},\mathbf{l})\,\theta(k,l,j)Q(l)[Q(j)-Q(k)], \tag{A1}$$

where

$$\theta(k,j,l)=\frac{1}{\omega(k)+\omega(j)+\omega(l)} \tag{A2}$$

and

$$B(\mathbf{j},\mathbf{k},\mathbf{l})=L(\mathbf{k},\mathbf{k}-\mathbf{l})=\frac{k^4-2k^3l\mu+kl^3\mu}{|\mathbf{k}-\mathbf{l}|^2}(1-\mu^2), \tag{A3}$$

as given by (E24), where $\mu$ is a directional cosine between $\mathbf{k}$ and $\mathbf{l}$. Then the energy transfer rate $T(k)$ becomes

$$T(k)=4\pi k^2\int d^3l\,L(\mathbf{k},\mathbf{k}-\mathbf{l})\,\theta(k,|\mathbf{k}-\mathbf{l}|,l)Q(l)[Q(|\mathbf{k}-\mathbf{l}|)-Q(k)]. \tag{A4}$$

For the numerical computation it is convenient to use the integration variables $l$ and $j$ instead of $l$ and $\mu$,

$$\mu=\frac{k^2+l^2-j^2}{2kl}\rightarrow d\mu=-\frac{j}{kl}dj. \tag{A5}$$

[5]We believe that this can be proved; but, at worst, arguments can be put forward to suggest that this is the case.

In this notation

$$1-\mu^2=\frac{1}{4k^2l^2}(k+l+j)(k+l-j)(k-l+j)(l+j-k),$$

$$k^4-2k^3l\mu+kl^3\mu=(1/2)[2k^2j^2+l^2(l^2-k^2-j^2)].$$

Then $L(\mathbf{k},\mathbf{k}-\mathbf{l})$ can be expressed as

$$L(\mathbf{k},\mathbf{k}-\mathbf{l})=\frac{1}{8k^2l^2j^2}H(k,l,j)I(k,l,j), \tag{A6}$$

where

$$H(k,l,j)=2k^2j^2+l^2(l^2-k^2-j^2), \tag{A7}$$

$$I(k,l,j)=(k+l+j)(k+l-j)(k-l+j)(l+j-k). \tag{A8}$$

Substituting Eqs. (A5) and (A6) into Eq. (A4) yields

$$T(k)=\frac{\pi^2}{k}\int dl\int dj\,\frac{1}{lj}H(k,l,j)I(k,l,j)\,\theta(k,j,l)Q(l)[Q(j)-Q(k)]. \tag{A9}$$

Since $k$, $j$, and $l$ make a triangle, the integration region for $l$ and $j$ is bounded to

$$l+j\geqslant k,\quad j+k\geqslant l\geqslant j-k. \tag{A10}$$

In the above we employ $l,j$ instead of $l$, $\mu$, as this is more convenient for our present work.

## APPENDIX B: EVALUATION OF THE KOLMOGOROV CONSTANT AS A CONSISTENCY CHECK

At this point we make a digression: can we determine the Kolmogorov constant? One way of determining the viscosity is to make use of Eq. (5.8):

$$\nu(k|k_c)=-\frac{(C^2\varepsilon/\sigma k_c)T(x)}{2K_0\varepsilon^{2/3}k^{1/3}}=-\frac{C^2\varepsilon^{1/3}}{2K_0\sigma}k_c^{-4/3}\frac{T(x)}{x^{1/3}}. \tag{B1}$$

The present numerical calculation gives $T(x)/x^{1/3}=-1.22$ in the asymptotic region. Substituting this and $C=K_0/4$ into Eq. (B1) yields

$$\nu(k|k_c)=\frac{1.22K_0\varepsilon^{1/3}}{32\sigma}k_c^{-4/3}. \tag{B2}$$

The frequency defined in Eq. (5.3) is just $\nu(k|k_c)k^2$, so that

$$\sigma=\frac{1.22K_0}{32\sigma}. \tag{B3}$$

Combining Eq. (5.18) with Eq. (B3) yields

$$K_0=1.65,\quad \sigma=0.25, \tag{B4}$$

which agree with currently trusted values.

## APPENDIX C: NUMERICAL CONVERGENCE OF $T_{cross}(k|k_c)$

The integration region is regions 1 and 2 in Fig. 3. Since $Q(l)\sim l^{-11/3}$, we have to be careful with the integration in the vicinity of $l\approx 0$ and $j\approx 0$; this situation is realized only when $k\approx k_c$.

### 1. $l\to 0$

The dangerous region is around $P_2$ in Fig. 3, which is specified as

$$l+k\geqslant j\geqslant k_c,\quad k_c\geqslant l\geqslant k_c-k. \tag{C1}$$

Since we are interested in the integration coming from $l\approx k-k_c\approx 0$, a new variable $j=t+k$ is introduced in place of $j$. Then the region (C1) is changed to

$$l\geqslant t\geqslant \delta,\quad k_c\geqslant l\geqslant \delta, \tag{C2}$$

where $\delta$ is defined as

$$\delta=k_c-k, \tag{C3}$$

so that $\delta$ is regarded as small. We substitute $j=k+t$ into various terms in Eq. (3.2) to retain the highest term only:

$$H=2k^4,\ \ I=4k^2(l^2-t^2),\quad \theta=\frac{1}{2\omega(k)},$$

$$\frac{1}{j}=\frac{1}{k}, \quad Q(j)-Q(k)=tQ'(k). \tag{C4}$$

Then Eq. (3.8) becomes

$$T_{cross}(k|k_c)=\frac{4\pi^2k^4Q'(k)}{\omega(k)}\int_\delta dl\,\frac{Q(l)}{l}\int_\delta^l dt(l^2-t^2)t$$
$$=\frac{\pi^2k^4Q'(k)}{\omega(k)}\int_\delta dl\,\frac{Q(l)}{l}(-2l^2\delta^2+\delta^4+l^4). \tag{C5}$$

If we use $Q(l)\sim l^{-11/3}$, the contribution from the lower bound $\delta$ becomes $(114/55)\delta^{1/3}$, implying no divergence at all. The numerical calculation can be safely carried out.

### 2. $j\to 0$

Here we are concerned with the region around point $P_1$ in Fig. 3. If we introduce a new variable such as $l=t+k$, the integration region is specified by

$$j\geqslant t\geqslant\delta, \quad k_c\geqslant j\geqslant\delta. \tag{C6}$$

Under this situation

$$H=2k^3t, \quad I=4k^2(j^2-t^2), \quad \theta=\frac{1}{2\omega(k)},$$
$$\frac{1}{l}=\frac{1}{k}, \quad Q(l)=Q(k). \tag{C7}$$

Then Eq. (3.8) becomes

$$T_{cross}(k|k_c)=\frac{4\pi^2k^3Q(k)}{\omega(k)}\int_\delta dj\,\frac{Q(j)-Q(k)}{j}\int_\delta^j dt(j^2-t^2)t$$
$$=\frac{\pi^2k^3Q(k)}{\omega(k)}\int_\delta dj\frac{Q(j)-Q(k)}{j}$$
$$\times(-2j^2\delta^2+\delta^4+j^4). \tag{C8}$$

Again the divergence at $j\approx 0$ does not occur.

## APPENDIX D: ENERGY TRANSFER RATE ACROSS $k_c$

Notice that $T(k,l,j)$ in Eq. (3.2) is antisymmetric under the exchange of $k$ and $j$. However, it is not symmetric under the exchange of $j$ and $l$. In order to confirm the energy conservation, it is helpful to introduce the symmetric transfer rate $\tilde{T}(k,l,j)$:

$$\tilde{T}(k,l,j)=\frac{I(k,l,j)\,\theta(k,l,j)}{2kjl}\{[H(k,l,j)+H(k,j,l)]$$
$$\times Q(l)Q(j)-[H(k,l,j)Q(l)$$
$$+H(k,j,l)Q(j)]Q(k)\}. \tag{D1}$$

With this definition it is easy to show that

$$\tilde{T}(k,l,j)+\tilde{T}(j,k,l)+\tilde{T}(l,j,k)=0. \tag{D2}$$

Note that the above identity holds irrespective of where $k$, $l$, and $j$ are located. It means that if $\tilde{T}(k,l,j)$ is approximated in a certain way, it must satisfy Eq. (D2) as far as the energy conservation is concerned.

Using Eq. (D1) the energy transfer rate across $k_c$ is written as

$$-\Pi(k_c)=\int_0^{k_c}dk\left[\int_0^{k_c}dl\int_0^{k_c}dj+\int_0^{k_c}dl\int_{k_c}^{k_{max}}dj\right.$$
$$\left.+\int_{k_c}^{k_{max}}dl\int_0^{k_c}dj+\int_{k_c}^{k_{max}}dl\int_{k_c}^{k_{max}}dj\right]\tilde{T}(k,l,j). \tag{D3}$$

The first integration in Eq. (D3) vanishes because $k$, $l$, $j$ are located in the same wave number region. In the second integral the dummy variables $k$ and $j$ are exchanged, while in the third one $k$ and $l$ are exchanged:

$$\int_0^{k_c}dk\int_0^{k_c}dl\int_{k_c}^{k_{max}}dj\tilde{T}(k,l,j)+\int_0^{k_c}dk\int_{k_c}^{k_{max}}dl\int_0^{k_c}dj\tilde{T}(k,l,j)$$
$$=\int_0^{k_c}dj\int_0^{k_c}dl\int_{k_c}^{k_{max}}dk\tilde{T}(j,l,k)+\int_0^{k_c}dl\int_{k_c}^{k_{max}}dk\int_0^{k_c}dj\tilde{T}(l,k,j)$$
$$=\int_{k_c}^{k_{max}}dk\int_0^{k_c}dl\int_0^{k_c}dj[\tilde{T}(j,l,k)+\tilde{T}(l,k,j)]$$
$$=-\int_{k_c}^{k_{max}}dk\int_0^{k_c}dl\int_0^{k_c}dj\tilde{T}(k,l,j). \tag{D4}$$

In deriving the last line we have used Eq. (D2). If $\tilde{T}(k,l,j)$ is approximated in a wrong way, there will be no guarantee that the second line of Eq. (D4) is the same as the last line.

Finally, we have the flux $\Pi(k_c)$ defined as

$$\Pi(k_c)=\left[\int_{k_c}^{k_{max}}dk\int_0^{k_c}dl\int_0^{k_c}dj-\int_0^{k_c}dk\int_{k_c}^{k_{max}}dl\int_{k_c}^{k_{max}}dj\right]\tilde{T}(k,l,j). \tag{D5}$$

Since the integration regions over $l$ and $j$ are symmetric in Eq. (D5), we can replace the symmetrized transfer rate $\tilde{T}$ by an orginal one $T$:

$$\Pi(k_c)=\left[\int_{k_c}^{k_{max}}dk\int_0^{k_c}dl\int_0^{k_c}dj-\int_0^{k_c}dk\int_{k_c}^{k_{max}}dl\int_{k_c}^{k_{max}}dj\right]T(k,l,j). \tag{D6}$$


[1] W.D. McComb and C. Johnston, Physica A **292**, 346 (2001).
[2] D. Forster, D.R. Nelson, and M.J. Stephen, Phys. Rev. A **16**, 732 (1977).
[3] G.L. Eyink, Phys. Fluids **6**, 3063 (1994).
[4] S.F. Edwards, J. Fluid Mech. **18**, 239 (1964).
[5] W. D. McComb, *The Physics of Fluid Turbulence* (Oxford University Press, New York, 1990).
[6] W.D. McComb, Rep. Prog. Phys. **58**, 1117 (1995).
[7] J.P. Bouchaud and M.E. Cates, Phys. Rev. E **48**, 635 (1993).
[8] B. Vreman, B. Geurts, and H. Kuerten, J. Fluid Mech. **278**, 351 (1994).
[9] B.J. Geurts, Phys. Fluids **9**, 3585 (1997).
[10] W.D. McComb, A. Hunter, and C. Johnston, Phys. Fluids **13**, 2030 (2001).
[11] L. Machiels, Phys. Rev. Lett. **79**, 3411 (1997).
[12] A.J. Young and W.D. McComb, J. Phys. A **33**, 133 (2000).
[13] W.D. McComb and C. Johnston, J. Phys. A **33**, L15 (2000).
[14] J-P. Chollet and M. Lesieur, J. Atmos. Sci. **38**, 2747 (1981).
[15] R.H. Kraichnan, J. Atmos. Sci. **33**, 1521 (1976).
[16] J.A. Domeradzki, R.W. Metcalfe, R.S. Rogallo, and J.J. Riley, Phys. Rev. Lett. **58**, 547 (1987).
[17] R.H. Kraichnan, J. Fluid Mech. **47**, 3 (1971).
[18] K. Ohkitani and S. Kida, Phys. Fluids A **4**, 794 (1992).